Repellons as Dark Energy: A Brane-Based Microphysical Model for Cosmic Acceleration and Void Dynamics

Hari Kumar Nair

Toronto, CANADA

Email: harismind@gmail.com

LinkedIn: https://www.linkedin.com/in/hari-kumar-0068462b

This preprint is also available on Zenodo: DOI: **10.5281/zenodo.17914713**

Abstract

Observations of Type Ia supernovae, the cosmic microwave background, and baryon acoustic oscillations indicate that the Universe is undergoing accelerated expansion. In ΛCDM, this is attributed to a cosmological constant Λ. While successful, Λ lacks a microphysical origin, and alternative dynamical models often treat dark energy as a structureless homogeneous fluid. We explore a concrete alternative hypothesis: that dark energy arises from an ensemble of discrete brane-like objects, "repellons," modelled as closed two-dimensional shells embedded in three-dimensional space. We ground this hypothesis in general relativity using a relativistic thin-shell model, demonstrating how tension-dominated branes can source an effectively repulsive gravitational potential.

The repellon brane contributes stress–energy to our spacetime while its interior is not part of the observable Universe. When coarse-grained over cosmological volumes, the ensemble behaves as an effective fluid with equation-of-state parameter $\omega_R < -1/3$, capable of driving late-time acceleration. We retain standard baryons and cold dark matter as the agents of structure formation and halo dynamics, treating repellons purely as a dark-energy sector. Motivated by a simple gravitational-response picture, we further posit a mild anti-correlation between repellon and matter densities, such that repellons preferentially populate underdense regions. Numerical integration of the coupled linear perturbation equations confirms this mechanism, showing that repellons naturally accumulate in voids as matter evacuates. We outline how this void bias could enhance void expansion and modify large-scale flows and late-time ISW correlations relative to ΛCDM with the same background history. This framework is phenomenological, designed to identify qualitative signatures (specifically in void dynamics) that can guide future perturbative calculations and N-body simulations.

Key Words: Astrophysics, Dark Energy, Cosmology, Cosmic Acceleration, Brane Cosmology, Repellon, Cosmic Voids, Large-scale Structure, Integrated Sachs-Wolfe Effect, ΛCDM, Dark Matter, String Theory

Contents

1 Introduction

Over the past two decades, multiple lines of evidence have established that the expansion of the Universe is accelerating. Type Ia supernova distance–redshift measurements [1, 2, 18] the angular scale of acoustic peaks in the CMB, and baryon acoustic oscillations (BAO) [3, 4] collectively point to a late-time component with large negative pressure. In the standard ΛCDM model this is encoded in a cosmological constant with equation-of-state parameter $\omega = -1$. Despite its empirical success, Λ raises long-standing theoretical puzzles, including the small but nonzero value of the inferred vacuum energy density and the absence of a compelling microphysical explanation.

A broad family of alternatives replaces Λ [4, 5] with dynamical dark energy—typically a scalar field or effective fluid whose equation of state may deviate from -1 and evolve with time. Modified-gravity approaches pursue a different route by changing the gravitational sector itself. In most cases, however, the accelerated-expansion component is still treated as a phenomenological background with limited guidance on what, if anything, the dark-energy sector is "made of." This motivates exploring concrete microphysical pictures that reproduce familiar background behaviour while offering new, falsifiable structure-based signatures.

In this work we investigate one such hypothesis: that dark energy arises from a population of discrete, brane-like objects embedded in ordinary three-dimensional space. We call these objects **repellons**. By construction, a repellon is a closed two-dimensional surface (topologically spherical) whose brane carries energy and tension, while its enclosed "interior" does not belong to our Universe. From the viewpoint of general relativity, the stress–energy of a large ensemble of such shells can be coarse-grained into an effective fluid description. We adopt the central working assumption that this effective repellon fluid has an equation-of-state parameter $\omega_R < -1/3$, satisfying the standard condition for driving accelerated expansion in an FRW universe.

For $\omega_R \approx -1$, the model becomes nearly indistinguishable from ΛCDM at the background level while providing a distinct microphysical interpretation.

A key scope decision in this paper is to **separate the roles of dark matter and repellons**. We do not attempt to explain galactic or cluster-scale dark-matter phenomena with repellons. Instead, we retain the standard matter sector (baryons plus cold dark matter) as the driver of structure formation and halo dynamics, with effective $\omega_M \approx 0$. Repellons are introduced solely as a dark-energy-like

component that enters the Einstein–Friedmann equations in the usual way. This choice is both conservative and strategically clarifying: it preserves the well-tested successes of CDM on small and intermediate scales while allowing the repellon hypothesis to be evaluated primarily through its impact on late-time expansion and large-scale underdense environments.

Beyond homogeneous expansion, the repellon hypothesis carries a distinctive, testable expectation about spatial distribution. At the microscopic level, we assume repellons are gravitationally repelled by high matter densities while weakly attracting one another. Coarse-grained on large scales, this implies a **mild anti-correlation** between matter and repellon densities: repellons preferentially occupy underdense regions (cosmic voids) while avoiding the interiors of halos, galaxies, and clusters. This void-filling tendency is qualitatively reminiscent of how dark energy becomes dynamically important in low-density regions, but here it is tied to a discrete-object microphysics rather than a featureless vacuum component.

The combination of negative pressure and void preference suggests a dual cosmological role. On the one hand, repellons act as an effective dark-energy fluid in the homogeneous Friedmann equations, producing late-time acceleration. On the other hand, as quantified by the linear perturbation equations in Section 4, a mild enhancement of the local repellon fraction inside voids may subtly modify void growth, large-scale peculiar velocities, and late-time ISW correlations relative to ΛCDM with the same background expansion history. We emphasise that our treatment of this second aspect is deliberately **phenomenological**: rather than deriving perturbation-level bias from a fully specified brane action, we encode it through minimal parameters that can be constrained or falsified by future data and simulations. These parameters are incorporated into the linear perturbation equations derived in Section 4, providing a framework for future numerical studies.

Accordingly, the goals of this paper are modest but concrete. We

(i) set out a minimal FRW framework in which the repellon sector replaces Λ through a constant ω_R effective fluid;

(ii) articulate a simple, physically motivated parameterisation of repellon–matter anti-correlation relevant to void-scale dynamics; and

(iii) derive linear perturbation equations in Section 4 and outline observational signatures—particularly in void profiles, boundary flows, and late-time ISW

correlations—that could, in principle, distinguish a repellon cosmology from a pure cosmological constant and from generic dark-energy parameterisations. A more fundamental field-theoretic embedding is left to future work, while a quantitative linear perturbation analysis is presented in Section 4.

2 Repellons as an Effective Dark-Energy Fluid

2.1 FRW background with a repellon component

We assume a standard, homogeneous and isotropic universe with FRW metric (setting $c = 1$):

$$s^2 = -dt^2 + a^2(t)\left[\frac{dr^2}{1-kr^2} + r^2 d\Omega^2\right] \tag{2.1}$$

where $a(t)$ is the scale factor and $k = 0, \pm 1$ is the spatial curvature.

We include four energy components:

- Baryons: density ρ_b, equation of state $\omega_b = 0$,
- Cold dark matter (CDM): density ρ_c, equation of state $\omega_c = 0$,
- Radiation: density ρ_r, equation of state $\omega_r = 1/3$,
- Repellon fluid: density ρ_R, equation of state

$$p_R = \omega_R \rho_R, \qquad \omega_R < -\frac{1}{3} \tag{2.2}$$

On cosmological scales, we assume the repellon fluid is approximately **homogeneous**: it does not significantly clump on galaxy scales and its density can be treated as smooth, with mild spatial variations that are discussed later in connection with voids.

The total energy density is

$$\rho_{\text{tot}} = \rho_b + \rho_c + \rho_r + \rho_R \tag{2.3}$$

With the standard Einstein equation

$$G_{\mu\nu} = 8\pi G T_{\mu\nu}$$

and total stress-energy tensor $T_{\mu\nu} = \sum_i T_{\mu\nu}^{(i)}$, the FRW background equations are the usual Friedmann equations.

The **first Friedmann equation** (expansion rate) is

$$H^2 \equiv \left(\frac{\dot{a}}{a}\right)^2 = \frac{8\pi G}{3}\rho_{\text{tot}} - \frac{k}{a^2} = \frac{8\pi G}{3}(\rho_b + \rho_c + \rho_r + \rho_R) - \frac{k}{a^2} \tag{2.4}$$

The **acceleration equation** is

$$\frac{\ddot{a}}{a} = -\frac{4\pi G}{3}(\rho_{\text{tot}} + 3p_{\text{tot}}) = -\frac{4\pi G}{3}\left[(\rho_b + \rho_c + \rho_r + \rho_R) + 3\left(0 + 0 + \frac{1}{3}\rho_r + \omega_R\rho_R\right)\right]$$

which simplifies to

$$\frac{\ddot{a}}{a} = -\frac{4\pi G}{3}[\rho_b + \rho_c + 2\rho_r + \rho_R(1 + 3\omega_R)] \tag{2.5}$$

The **repellon contribution** to acceleration is the term $\rho_R(1 + 3\omega_R)$. Since $\rho_R > 0$, accelerated expansion ($\ddot{a} > 0$) requires

$$\rho_R(1 + 3\omega_R) < 0 \Rightarrow \omega_R < -\frac{1}{3} \tag{2.6}$$

Thus, the condition for repellons to drive cosmic acceleration is identical to the usual dark-energy condition: an effective equation of state less than $-1/3$.

2.2 Evolution of energy densities and special cases

Assuming no non-gravitational couplings between the fluids, each component satisfies its own continuity equation,

$$\dot{\rho}_i + 3H(\rho_i + p_i) = 0 \tag{2.7}$$

For constant ω_i, this integrates to

$$\rho_i(a) = \rho_{i0} a^{-3(1+\omega_i)} \tag{2.8}$$

Thus,

$$\rho_b(a) \propto a^{-3} \tag{2.9}$$

$$\rho_c(a) \propto a^{-3} \tag{2.10}$$

$$\rho_r(a) \propto a^{-4} \tag{2.11}$$

$$\rho_R(a) \propto a^{-3(1+\omega_R)} \tag{2.12}$$

Special cases for the repellon fluid:

- $\omega_R = -1: \rho_R(a) = \rho_{R0}$ is constant. The repellon fluid is dynamically indistinguishable at the background level from a cosmological constant. (See Section 3.3 for the microphysical derivation of this constant-density behavior via continuous repellon creation.)
- $-1 < \omega_R < -1/3: \rho_R(a)$ slowly decays with the expansion but eventually dominates over matter, yielding a form of dynamical dark energy similar to quintessence.
- For $\omega_R < -1$ (the phantom regime), $\rho_R(a)$ grows with time. While not excluded by data, we focus on the non-phantom regime to avoid the theoretical pathologies associated with future singularities (Big Rip) though it is not excluded a priori by the phenomenological setup.

For concreteness, we focus on a spatially flat universe ($k = 0$) at late times, with present-day density parameters

$$\Omega_{b0} = \frac{8\pi G\rho_{b0}}{3H_0^2}, \tag{2.13}$$

$$\Omega_{c0} = \frac{8\pi G\rho_{c0}}{3H_0^2}, \tag{2.14}$$

$$\Omega_{r0} = \frac{8\pi G\rho_{r0}}{3H_0^2}, \tag{2.15}$$

$$\Omega_{R0} = \frac{8\pi G\rho_{R0}}{3H_0^2}, \tag{2.16}$$

Satisfying

$$\Omega_{b0} + \Omega_{c0} + \Omega_{r0} + \Omega_{R0} = 1 \tag{2.17}$$

Defining $\Omega_{m0} = \Omega_{b0} + \Omega_{c0}$, the Hubble parameter becomes

$$H^2(a) = H_0^2\left[\Omega_{r0}a^{-4} + \Omega_{m0}a^{-3} + \Omega_{R0}a^{-3(1+\omega_R)}\right] \tag{2.18}$$

At early times ($a \ll 1$), the radiation and matter terms dominate; the universe undergoes the standard radiation-dominated and matter-dominated phases. At late times, the repellon term takes over and drives accelerated expansion. For $\omega_R \simeq -1$, the background expansion history is very close to ΛCDM, with the cosmological constant replaced by a nearly constant repellon energy density.

Microscopically, individual repellons are envisioned as closed 2-dimensional brane-like shells which, when averaged over cosmological volumes, give rise to the effective fluid described above. The repulsive character of repellons manifests itself in two ways: through their negative pressure at the homogeneous level (encoded in $\omega_R < -1/3$), and through a tendency to avoid high-density regions of baryons and dark matter, preferentially populating voids and underdense regions. In what follows we treat the repellon fluid as homogeneous at the FRW background level, with its void preference entering only as a perturbative, large-scale effect discussed in Section 3.

3 Deriving Repellon Properties from the Brane Action

In this section, we derive the key physical properties of repellons—negative gravitational mass, decoupled inertial mass, and the effective equation of state $\omega_R < -1/3$—starting from a fundamental brane action. This provides a microphysical embedding for the phenomenological fluid description introduced earlier, grounding the model in string-inspired brane theory while ensuring compatibility with general relativity (GR).

3.1 The Nambu-Goto Action for a Closed 2-Brane [6]

We model each repellon as a closed, microscopic 2-brane (topologically a sphere) embedded in our 4D spacetime (3 spatial + 1 time dimension). The simplest action for such a brane is the Nambu-Goto action, which generalizes the relativistic point particle or string action to higher-dimensional objects:

$$S = -T \int d^3\xi \sqrt{-\det\left(g_{ab}\right)} \tag{3.1}$$

where:

- $T > 0$ is the brane tension (energy per unit area, with dimensions of mass/volume in natural units),
- $\xi^a (a = 0,1,2)$ are the worldvolume coordinates parameterizing the brane's 3D worldsheet,
- $g_{ab} = \partial_a X^\mu \, \partial_b X^\nu G_{\mu\nu}$ is the induced metric on the worldvolume,
- $X^\mu(\xi)$ are the embedding functions mapping the worldvolume to the bulk spacetime coordinates,
- $G_{\mu\nu}$ is the bulk metric (assumed Minkowski or weakly curved for local analysis).

This action represents the worldvolume "area" swept by the brane, minimized for classical solutions (analogous to geodesics). For a static, spherical repellon of radius R, the spatial area is $4\pi R^2$, so the rest energy contributed by the brane is $E_{\text{brane}} = T \times 4\pi R^2$. The sign $-T$ ensures positive energy for timelike worldsheets.

To incorporate fields or interior matter (as per the model's "inner universe"), we can extend to the Dirac-Born-Infeld (DBI) action, but for minimalism, we stick to Nambu-Goto + tension, assuming negligible gauge fields or dilaton variations (common in type IIA string theory for D2-branes).

3.2 Stress-Energy Tensor [7] and Effective Equation of State

The repellon's contribution to spacetime curvature comes from its stress-energy tensor, derived by varying the action with respect to the bulk metric $G_{\mu\nu}$:

$$T^{\mu\nu}(x) = \frac{2}{\sqrt{-G}}\frac{\delta S}{\delta G_{\mu\nu}} = T\int d^3\xi\,\sqrt{-g}\,g^{ab}\,\partial_a X^\mu\,\partial_b X^\nu\,\frac{\delta^{(4)}\big(x - X(\xi)\big)}{\sqrt{-G}} \tag{3.2}$$

where $\delta^{(4)}$localizes the energy-momentum on the brane worldsheet. On the worldvolume itself, the surface stress-energy tensor is:

$$S^{ab} = -Tg^{ab} \tag{3.3}$$

corresponding to surface energy density $\sigma = T$ and isotropic surface pressure $p_s = -T$ (i.e., equation of state $\omega_{\text{brane}} = p_s/\sigma = -1$ on the brane, like a 2D cosmological constant).

For a single repellon, this describes a thin shell with tension-driven negative pressure. However, in cosmology, we consider an ensemble of many microscopic repellons, coarse-grained over large volumes to form an effective fluid with density ρ_R and pressure p_R, where $\omega_R = p_R/\rho_R$.

To derive ω_R, we treat the ensemble as a gas or network of 2-branes (domain walls in 3D space). In defect cosmology, the average stress-energy for non-interacting p-branes in d=3 spatial dimensions is anisotropic: pressure $p = -\rho$ along the p tangential directions (due to tension), and $p = 0$ in the (3-p) transverse directions. For perturbations, we assume an effective sound speed $c_{s,R}^2 = 0$ to allow mild clustering on void scales, consistent with the brane tension. Isotropizing over random orientations yields:

$$\omega = -\frac{p}{3} \tag{3.4}$$

For p=2 (repellons as 2-branes):

$$\omega_R = -\frac{2}{3} \tag{3.5}$$

For a static 2-brane, $T_\mu^\mu = 3\rho_R$ (energy + two negative pressures), leading to $\omega_R = -2/3$.

If the repellons have average velocity v (e.g., due to quantum fluctuations or cosmic flows), the equation of state generalizes to:

$$\omega_R = v^2 - \frac{2}{3} \tag{3.6}$$

with $v \approx 0$ yielding $\omega_R = -2/3 < -1/3$, sufficient for accelerated expansion ($\rho_R + 3p_R = \rho_R(1 + 3\omega_R) = -\rho_R < 0$).

For $\omega_R \approx -1$, we postulate that the continuous creation of repellons via quantum fluctuations maintains a constant ρ_R, effectively mimicking vacuum energy. This is consistent with steady-state models or quintessence with particle production. This effective fluid description sets the stage for the linear perturbation equations in Section 4, where we explore how repellon fluctuations couple to matter and influence void dynamics.

3.3 Repellon Creation Mechanism

The repellon ensemble is modeled as a network of closed 2-branes with an intrinsic equation of state $\omega_{int} = -2/3$, arising from the averaging of anisotropic tension. In the absence of source terms, the continuity equation implies the density would dilute as $\rho_R \propto a^{-1}$. To reconcile this with the phenomenological requirement of an effective $\omega_{eff} \approx -1$ (constant energy density), we postulate a continuous creation of repellons driven by the expansion of the universe.

We modify the continuity equation to include an energy injection rate $\boldsymbol{\mathcal{C}}$:

$$\dot{\rho_R} + 3H(\rho_R + p_R) = \boldsymbol{\mathcal{C}} \tag{3.7}$$

Substituting $p_R = -\frac{2}{3}\rho_R$, the condition for constant density ($\dot{\rho_R} = 0$) requires:

$$\boldsymbol{\mathcal{C}} = 3H\left(\rho_R - \frac{2}{3}\rho_R\right) = H\rho_R \tag{3.8}$$

Physical Interpretation:

This creation rate $\boldsymbol{\mathcal{C}} \propto H\rho_R$ suggests that repellon nucleation is driven by vacuum fluctuations in the expanding spacetime, analogous to Schwinger pair production in a de Sitter background. We interpret this not as a violation of conservation, but as an energy transfer from the gravitational field to the repellon sector. The Hubble scale H^{-1} provides the natural horizon size for these fluctuations. Furthermore, the rapid cosmic expansion causally separates nucleated brane-antibrane pairs, preventing immediate annihilation and allowing a net accumulation of repellon density.

This mechanism bridges the gap between the microphysical brane tension ($\omega_{int} = -2/3$) and the macroscopic dark energy behavior ($\omega_{eff} \approx -1$).

3.4 Thin-shell toy model and effective gravitational mass

To make the "repellon as a closed 2-brane" picture more concrete, it is useful to look at a simple thin-shell toy model in general relativity. We consider a static, spherically symmetric shell at areal radius R separating a flat interior from a Schwarzschild exterior. This is the standard Darmois–Israel junction setup; details are collected in Appendix A.

The spacetime inside the shell ($r < R$) is taken to be exactly Minkowski,

$$\mathrm{d}s_-^2 = -\mathrm{d}t_-^2 + \mathrm{d}r^2 + r^2\,\mathrm{d}\Omega^2 \tag{3.9}$$

while the exterior ($r > R$) is Schwarzschild with mass parameter M,

$$\mathrm{d}s_+^2 = -\left(1 - \frac{2GM}{r}\right)\mathrm{d}t_+^2 + \left(1 - \frac{2GM}{r}\right)^{-1}\mathrm{d}r^2 + r^2\,\mathrm{d}\Omega^2 \tag{3.10}$$

By Birkhoff's theorem, the parameter M is precisely the total gravitational mass felt by distant test particles.

The Israel junction conditions relate the jump in extrinsic curvature across the shell to its surface stress–energy tensor $S^a{}_b$. Assuming a perfect 2D fluid on the shell,

$$S^a{}_b = \mathrm{diag}(-\sigma, p, p) \tag{3.11}$$

with surface energy density σ and isotropic surface pressure p (tension corresponds to $p < 0$), one finds the standard expressions (see Appendix A)

$$\sigma = -\frac{1}{4\pi GR}\left(\sqrt{f_+(R)} - \sqrt{f_-(R)}\right), \qquad f_\pm(R) \equiv -g_{tt}^{\pm}(R) \tag{3.12}$$

and a similar expression for p. For the present Minkowski–to–Schwarzschild case we have $f_-(R) = 1$ and

$$f_+(R) = 1 - \frac{2GM}{R} \equiv 1 - \mu \tag{3.13}$$

where $\mu \equiv 2GM/R$ is the compactness of the shell.

For $0 < \mu < 1$ (positive mass parameter, shell outside its Schwarzschild radius), we obtain

$$\sigma(\mu) = \frac{1}{4\pi GR}(1 - \sqrt{1-\mu}) > 0 \tag{3.14}$$

so the shell has positive surface energy density. The proper rest mass of the shell is then

$$m_{\mathrm{shell}} \equiv 4\pi R^2 \sigma = \frac{R}{G}(1 - \sqrt{1-\mu}) \tag{3.15}$$

which for $\mu \ll 1$ admits the expansion

$$m_{\mathrm{shell}} \approx M + \frac{GM^2}{2R} + \cdots \tag{3.16}$$

or, inverted,

$$M \approx m_{\text{shell}} - \frac{G m_{\text{shell}}^2}{2R} + \cdots \tag{3.17}$$

Thus the effective gravitational mass parameter M seen by distant observers is the shell's rest mass minus a negative gravitational binding-energy contribution. This is the familiar "mass deficit" of a strongly bound object in general relativity: gravitational self-energy reduces the effective mass compared with the naive sum of constituent rest masses.

One might hope to push this mechanism to the point where the effective gravitational mass becomes negative, $M < 0$, while maintaining positive surface energy density. However, in the simple Minkowski–to–Schwarzschild construction this turns out not to be possible with standard sign conventions. As shown explicitly in Appendix A, taking $M < 0$ forces

$$f_+(R) = 1 - \frac{2GM}{R} = 1 + \frac{2G\,|\,M\,|}{R} > 1, \qquad \sigma = \frac{1}{4\pi GR}\left(1 - \sqrt{1 + 2G\,|\,M\,|/R}\right) < 0 \tag{3.18}$$

so that the shell necessarily has $\sigma < 0$ and violates at least the weak and dominant energy conditions. In other words, within this particular toy model a genuinely repulsive Schwarzschild exterior ($M < 0$) requires "exotic" shell matter.

The lesson we take from this exercise is twofold. First, a closed 2-brane shell can carry its own effective gravitational mass parameter M that differs from its naive rest mass because of tension and gravitational binding effects. Second, obtaining an effective negative gravitational mass $M < 0$ in a static thin-shell configuration generically requires departures from classical energy-condition–respecting matter. In the present paper we therefore use the language of "negative gravitational mass" for repellons in an *effective* sense: M parametrises a repulsive exterior gravitational field sourced by brane-like stress-energy whose microphysical origin is left open, and whose detailed consistency with energy conditions is not imposed at the classical level. Appendix A makes this interpretation explicit in the simplest possible setting.

3.5 Effective equation of state and sound speed of the repellon fluid

On cosmological scales we treat the ensemble of repellons as a homogeneous and isotropic effective fluid with energy density ρ_R and pressure p_R, characterised at background level by an equation-of-state parameter

$$\omega_R \equiv \frac{p_R}{\rho_R} = \text{const.} \tag{3.19}$$

In Section 3.2 we argued, following the standard defect-network treatment of p-branes, that a static, randomly oriented network of 2-branes in three spatial dimensions has an average equation of state $\omega_R = -2/3$: the branes carry tension (negative pressure) along their two tangential directions and negligible pressure in the transverse direction, and isotropising over orientations yields $\omega = -p/3 = -2/3$ for $p = 2$. This "domain-wall value" provides a natural baseline for the repellon fluid.

In the late Universe, however, we do not expect the repellon network to be exactly static. Brane segments can move, annihilate, and be created; the network may interact weakly with the ambient expanding spacetime, and the ensemble-averaged stress–energy can deviate from the pure static-wall limit. Rather than attempting to model these microscopic processes in detail, we adopt a simple phenomenological parametrisation inspired by defect-network dynamics. We parameterize the intrinsic equation of state of the brane network as:

$$\omega_{int}(v^2) = v^2 - 2/3 \tag{3.20}$$

where v^2 represents the RMS velocity of the brane network. The static-network value $\omega_{int} = -2/3$ is recovered at $v^2 = 0$, while increasing v^2 makes the equation of state less negative.

However, as established in Section 3.3, the continuous creation of repellons modifies the macroscopic behavior of this fluid. While the constituent branes possess $\boldsymbol{\omega_{int} \geq -2/3}$, the energy injection from creation counteracts the dilution due to expansion, allowing the ensemble to mimic a fluid with an effective equation of state $\boldsymbol{\omega_R}$ much closer to -1.

Observationally, current data favour an effective dark-energy equation of state close to -1; in the cosmological applications below we therefore treat ω_R as a constant parameter in the range $-1 \leq \omega_R \leq -1/3$ **(representing a creation-dominated regime)**, with $\omega_R = -2/3$ as a physically motivated reference point for the underlying network dynamics.

To discuss perturbations in the repellon fluid we also need an effective sound speed c_s^2, defined in the usual way as the rest-frame derivative

$$c_s^2 \equiv \left.\frac{\delta p_R}{\delta \rho_R}\right|_{\text{rest}} \tag{3.21}$$

Without a fully specified microphysical action for the branes and their interactions, c_s^2 cannot be derived from first principles, and we therefore treat it as a phenomenological parameter subject to basic physical constraints: it should be positive (to avoid gradient instabilities) and subluminal (to avoid superluminal propagation in the effective theory),

$$0 < c_s^2 \leq 1 \tag{3.22}$$

As a simple illustrative choice, and to keep the fluid relatively smooth on small scales, we adopt the toy relation

$$c_s^2 = -\omega_R \tag{3.23}$$

in analogy with some barotropic dark-energy parameterisations. In the range of interest $-2/3 \leq \omega_R \leq -1/3$ this gives

$$\frac{1}{3} \leq c_s^2 \leq \frac{2}{3} \tag{3.24}$$

so the sound speed is positive and comfortably subluminal. This suppresses small-scale clustering of repellons and is consistent with the picture in which repellons primarily populate large underdense regions rather than forming compact bound structures.

We stress that the relations $\omega_R(v^2) = v^2 - 2/3$ and $c_s^2 = -\omega_R$ are introduced here purely as convenient phenomenological ansätze, guided by defect-network intuition rather than derived from

a specific microscopic brane model. A more complete treatment would start from an underlying action for the repellon sector, derive its stress–energy tensor and perturbation equations, and compute $\omega_R(a)$ and $c_s^2(a,k)$ self-consistently. In this paper we restrict ourselves to constant-ω_R and constant-c_s^2 toy models that capture the leading background effect of the repellon fluid and the qualitative expectation that repellons behave as a relatively smooth, tension-dominated component on cosmological scales.

3.6 Inertial versus gravitational mass for a composite repellon (toy picture)

The thin-shell toy model also helps clarify what we mean when we say that the "inertial" and "gravitational" masses of a composite repellon can differ.

Consider a repellon conceived as a closed 2-brane surrounding an inner region (the "inner universe") containing ordinary matter. Let $m_{\rm in} > 0$ denote the total rest mass of that interior matter, as measured by a comoving observer inside. This interior matter obeys the usual Newtonian relation $F = m_{\rm in} a$ in local inertial frames; in this sense $m_{\rm in}$ plays the role of an inertial mass.

The brane itself carries an energy density and tension encoded in its surface stress-energy $S^a{}_b$. For a spherical shell of radius R with surface energy density σ, the shell's proper rest mass is

$$m_{\rm shell} = 4\pi R^2 \sigma \tag{3.25}$$

so a simple bookkeeping of "constituent rest masses" would suggest an inertial mass

$$m_i \sim m_{\rm in} + m_{\rm shell} \tag{3.26}$$

However, what distant test particles respond to is not this naive sum, but the effective Schwarzschild mass parameter M appearing in the exterior metric. As we saw in the previous subsection and in Appendix A, M receives contributions not only from $m_{\rm in}$ and $m_{\rm shell}$, but also from gravitational binding energy and the detailed structure of the shell stress-energy (tension versus compression, anisotropies, etc.). Schematically one can think of

$$M = m_{\rm in} + m_{\rm shell} + E_{\rm grav} + \cdots \tag{3.27}$$

where E_{grav} is negative for a bound configuration. In a more exotic brane construction, additional contributions from higher-dimensional fields or vacuum polarisation could further shift M relative to m_i.

From a local viewpoint, the equivalence principle is not violated: freely falling observers in the vicinity of the brane or in the interior still see test particles follow geodesics, and local experiments cannot distinguish between inertial and gravitational mass. The "decoupling" we have in mind is instead a *global* one: for a composite extended object, the effective mass parameter M that sources curvature at large radii need not equal the naive inertial mass obtained by adding up the rest masses of its constituents. In particular, sufficiently exotic stress-energy on the shell can, in principle, drive M to values that differ dramatically from m_i, including the effective $M < 0$ regime discussed above, at the price of violating classical energy conditions.

In this paper we treat this thin-shell picture as a heuristic illustration of how repulsive effective gravity could arise from extended objects rather than as a fully realistic microphysical model. The cosmological analysis that follows is framed at the level of an effective fluid with equation-of-state parameter ω_R, sound speed c_s^2, and large-scale clustering properties motivated by brane physics but not derived from a specific microscopic action. A complete assessment of whether such composite objects can be realised in a stable, energy-condition–respecting theory—and whether their ensemble can consistently reproduce the desired repellon fluid—remains an open problem for future work.

4 Linear Perturbations in the Repellon Model

To move beyond the homogeneous FRW background and explore the impact of repellons on large-scale structure, particularly voids, we derive the linear perturbation equations for the repellon fluid. We treat repellons as a perfect fluid with constant equation-of-state parameter $\omega_R < -1/3$, coupled gravitationally to the matter sector (baryons + CDM, with $\omega_m = 0$). For simplicity, we focus on late times where radiation is negligible and assume a flat universe ($k = 0$).

We work in the Newtonian gauge for scalar perturbations, with the perturbed metric

$$ds^2 = a^2[-(1+2\Phi)d\tau^2 + (1-2\Psi)\delta_{ij}dx^i dx^j] \tag{4.1}$$

where τ is conformal time ($d\tau = dt/a$), $' = d/d\tau$, $\mathcal{H} = a'/a = aH$, and we assume no anisotropic stress so $\Psi = -\Phi$. In Fourier space with comoving wavenumber k, the perturbation variables are the density contrast $\delta_i = \delta\rho_i/\bar{\rho}_i$, velocity divergence $\theta_i = \nabla \cdot \mathbf{v}_i$ (comoving peculiar velocity), and pressure perturbation $\delta p_i = c_{s,i}^2 \delta\rho_i$.

Motivated by the brane microphysics (Section 3), we assume an effective sound speed $c_{s,R}^2 = 0$ for repellons to allow mild clustering on void scales (while $c_{s,m}^2 = 0$ for matter). Assuming no non-gravitational interactions, the fluids evolve via perturbed energy-momentum conservation.

The continuity equation [16] for each component i (R for repellons, m for matter) is

$$\delta_i' = -(1+\omega_i)(\theta_i + 3\Phi') - 3\mathcal{H}(c_{s,i}^2 - \omega_i)\delta_i \tag{4.2}$$

For repellons:

$$\delta_R' = -(1+\omega_R)(\theta_R + 3\Phi') - 3\mathcal{H}(-\omega_R)\delta_R \tag{4.3}$$

(since $c_{s,R}^2 = 0$).

The Euler equation is

$$\theta_i' = -\mathcal{H}(1-3\omega_i)\theta_i - \frac{c_{s,i}^2 k^2}{1+\omega_i}\delta_i - \frac{k^2\Phi}{1+\omega_i} \tag{4.4}$$

For repellons, incorporating the gravitational repulsion from matter (motivated by the void bias in Section 1), we modify the gravitational term to reflect negative effective coupling:

$$\theta_R' = -\mathcal{H}(1-3\omega_R)\theta_R - \frac{0\cdot k^2}{1+\omega_R}\delta_R + \frac{k^2\Phi}{1+\omega_R}. \tag{4.5}$$

(Note the positive sign on Φ, causing repellons to flow away from matter overdensities where $\Phi < 0$.) For matter:

$$\delta_m' = -\theta_m - 3\Phi', \qquad \theta_m' = -\mathcal{H}\theta_m - k^2\Phi \tag{4.6}$$

The components couple through the Einstein equations. The Poisson equation (sub-horizon approximation) is

$$k^2\Phi \approx -\frac{3}{2}\mathcal{H}^2(\Omega_m\delta_m + \Omega_R\delta_R(1+3\omega_R)) \tag{4.7}$$

where the repellon term $(1+3\omega_R) < 0$ sources a repulsive potential from $\delta_R > 0$.

This framework encodes the mild anti-correlation $\delta_R \approx b_R\delta_m$ with $b_R < 0$ (where b_R is a phenomenological bias parameter, typically $-0.1 \lesssim b_R < 0$), leading to enhanced void growth. Numerical solutions (e.g., via CLASS) can quantify deviations from ΛCDM, such as sharper void profiles and stronger late-time ISW signals, as discussed in subsequent sections. A full derivation from brane fluctuations remains for future work.

5 Repellons in Cosmic Voids

In the microscopic picture, individual repellons are closed 2-brane-like shells embedded in our universe, each enclosing an interior region that is not part of our spacetime. From the standpoint of large-scale cosmology, however, the more relevant question is how an ensemble of such objects distributes itself relative to baryons and cold dark matter. We therefore treat the repellon component phenomenologically, focusing on its large-scale bias and its role as an effective negative-pressure sector rather than on the detailed dynamics of any single brane.

At this level, we assume that repellons are effectively repelled by high densities of normal matter (including CDM), while exhibiting mutual attraction within their own sector. A natural consequence is that regions that are initially slightly overdense in matter tend to become slightly underdense in repellons, with the converse also holding. Over cosmic time, this mechanism produces a mild anti-correlation between matter and repellon densities, so that repellons preferentially occupy underdense regions and avoid the interiors of halos, galaxies, and clusters,

while remaining relatively smooth on very large scales. We parameterize this anti-correlation as $\delta_R \approx b_R \delta_m$with $b_R < 0$, which modifies the Euler equation as derived in Section 4.

This expectation is also consistent with the basic thin-shell intuition associated with tension-dominated closed branes: the stress-energy of a compact 2-surface can, in simple junction-condition reasoning, reduce the effective gravitational mass parameter experienced outside the object relative to a naive rest-mass estimate. While we do not rely on such a construction as a detailed microphysical derivation here, it provides a useful qualitative motivation for describing individual repellons as sourcing an effectively repulsive gravitational response. The cosmological analysis in this section, however, continues to be framed purely in terms of the coarse-grained repellon fluid and its large-scale bias.

In this picture, cosmic voids (the large underdense regions between filaments) [9, 10, 11, 17] become natural reservoirs for the repellon population. Within a void, the local matter density is below the cosmic mean, while the repellon density is plausibly at or slightly above its mean value. Because the repellon sector carries negative effective pressure (with equation-of-state parameter $\omega_R < -1/3$), its presence can enhance the local tendency of voids to expand relative to the background. In effect, repellon-enriched voids behave as mild local amplifiers of acceleration, potentially promoting more efficient evacuation of matter from their interiors than would occur in a standard matter-plus-Λ scenario with the same global expansion history.

This qualitative mechanism complements the homogeneous treatment of the previous section. On average, the repellon fluid acts as a dark-energy-like component responsible for late-time acceleration in the Friedmann equations. Superposed on this, its tendency to concentrate in voids rather than in filaments or halos suggests a distinctive imprint on void evolution and large-scale flows: regions already underdense in matter may experience an additional outward push associated with a higher local repellon fraction, sharpening the contrast between void interiors and the surrounding cosmic web.

A fully quantitative treatment of this possibility would require evolving coupled perturbations in both the matter and repellon sectors—for example by modifying Boltzmann solvers or by performing N-body simulations that include an additional dark-energy-like component whose perturbations are biased towards underdense regions. The linear perturbation equations in Section 4 provide the foundation for such a quantitative treatment. **A numerical integration of these**

equations confirming the anti-correlation and accumulation of repellons inside a growing void is presented in Appendix B.

6 Dark Matter, Halos, and the Separation of Roles

A crucial point in the present version of the repellon hypothesis is that **repellons are not intended to replace dark matter in galactic halos or clusters**. Instead, their primary role is to behave as a dark-energy-like component on large scales (with effective equation of state $\omega_R < -1/3$) and to influence void evolution by preferentially occupying underdense regions.

The evidence for dark matter in galaxies and clusters (including flat rotation curves, strong and weak gravitational lensing, and the dynamics of galaxy clusters) robustly points to the presence of additional **attractive** mass that is spatially correlated with the baryonic distribution, albeit more extended. In the simplest cold dark matter (CDM) scenario this is provided by a population of non-relativistic, positive-mass particles that cluster gravitationally and form halos.

If one attempted to make repellons also serve as dark matter, the required interaction pattern would be problematic: a component that is repelled by normal matter but attracted to itself tends, in simple Newtonian models, to **weaken or even reverse** the net gravitational pull on stars in the outer parts of galaxies and to reduce, rather than enhance, the lensing signal in clusters. Such behaviour is opposite to what is needed to explain dark-matter phenomena. In light of these issues, the present work adopts a more conservative stance:

- Dark matter is assumed to be **separate** from repellons and to behave in the usual way (cold, collisionless, attractive).
- Repellons are treated as a smooth, negative-pressure fluid that affects the expansion history and void dynamics but has **negligible impact on the internal structure of halos and galaxies**.

Operationally, this means that in the homogeneous Friedmann equations the matter sector includes both baryons and CDM, with total matter density $\rho_M = \rho_b + \rho_c$ and equation of state $\omega_M \approx 0$, while the repellon sector enters only through ρ_R and $\omega_R < -1/3$. On the scales of

individual galaxies and clusters, the local contribution of the repellon fluid to the gravitational potential is assumed to be extremely small compared with that of the matter distribution, just as in standard dark-energy models. In particular, the dark-matter interpretation of phenomena such as flat rotation curves and the lensing mass of systems like the Bullet Cluster remains unchanged; these are attributed to CDM halos rather than to repellon clumps.

This separation of roles has two advantages. First, it avoids the difficulties that arise when trying to use a repulsive component to mimic the strongly attractive behaviour of dark matter in bound systems. Second, it allows repellons to be constrained and tested primarily through their **dark-energy-like effects** (on the expansion history, void evolution, and large-scale flows) rather than through detailed fits to halo dynamics. In this sense, the repellon fluid should be viewed as a proposed microphysical interpretation of dark energy and void dynamics, complementing rather than replacing the existing dark matter paradigm.

7 Observational and Experimental Signatures

In the repellon-as-dark-energy picture developed above, the most direct signatures of repellons arise not from compact clumps or local laboratory effects, but from their influence on the **global expansion history** and on the **dynamics of large-scale structure**, especially voids.

Throughout this section we work with the effective-fluid description introduced in Section 3: an ensemble of repellons modelled as a homogeneous component with constant equation-of-state parameter (ω_R) and rest-frame sound speed (c_s^2). Motivated by the defect-network arguments of Section 3.2, we adopt ($-2/3 \leq \omega_R \leq -1/3$) as the natural range for a tension-dominated brane fluid, while observationally we are primarily interested in ($-1 \lesssim \omega_R \leq -1/3$), with ($\omega_R = -2/3$) as a reference value. For concreteness we take ($c_s^2 = -\omega_R$) in this section, so that ($1/3 \leq c_s^2 \leq 2/3$): the repellon fluid is smooth and only weakly clustered on sub-horizon scales, consistent with its role as a dark-energy–like component. Here we explore an alternative with $c_s^2 = -\omega_R$ for illustration; the baseline $c_s^2 = 0$ from Section 4 allows more clustering.

In this section we outline several observational avenues that could be used to test or constrain the repellon hypothesis.

7.1 Background expansion and the effective equation of state

At the homogeneous level, the repellon fluid behaves as a dark-energy-like component with constant or slowly varying effective equation-of-state parameter ω_R. As discussed in Section 2, the background evolution in a flat universe with matter and repellons is governed by

$$H^2(a) = H_0^2\left[\Omega_{r0}a^{-4} + \Omega_{m0}a^{-3} + \Omega_{R0}a^{-3(1+\omega_R)}\right] \tag{7.1}$$

where Ω_{R0} is the present-day repellon density fraction and $\omega_R < -1/3$. Observationally, the parameter combination (Ω_{R0}, ω_R) is already tightly constrained by Type Ia supernovae, baryon acoustic oscillations, and other distance–redshift measurements. In the simplest version of the repellon model, in which ω_R is constant, these observations can be used to directly bound the allowed repellon parameter space, just as they constrain phenomenological dark-energy models.

If future data continue to favour a value of ω_R extremely close to −1, the repellon fluid at the background level becomes nearly indistinguishable from a cosmological constant. In that regime, the most promising discriminants between the repellon picture and standard ΛCDM are not the background distances themselves, but the way in which voids and large-scale flows respond to a dark-energy component that is **microscopically structured** (in the form of brane-like repellons) and possibly biased towards low-density regions.

In practice, our cosmological implementation models the repellon sector as a 'clustering dark energy' fluid. While generic scalar field models often predict a relativistic sound speed ($c_s^2 \approx 1$) that suppresses sub-horizon growth, we adopt a vanishing effective sound speed, $c_{s,R}^2 \approx 0$, consistent with the perturbation analysis in Section 4. This choice is physically motivated by the heavy, discrete nature of the constituent branes, treating them effectively as a cold gas of extended objects rather than a relativistic wave. Crucially, a low sound speed lowers the Jeans length of the repellon fluid, allowing it to respond to gravitational potential gradients on cosmological scales. This enables the specific void-filling phenomenology proposed here: unlike a smooth cosmological constant, the repellon fluid can pile up in underdense regions, dynamically enhancing void evolution.

7.2 Void profiles and growth

As argued in Section 5, repellons are expected to preferentially populate underdense regions, enhancing the local acceleration of voids relative to the background. This suggests that the internal density profiles, shapes, and growth rates of cosmic voids may be sensitive probes of the repellon fluid. For example, in a repellon-enriched void one might expect:

1. Slightly faster evacuation of matter from the void interior compared with a ΛCDM void of the same initial depth.
2. Enhanced outward peculiar velocities of galaxies near void boundaries.
3. Modest modifications to the stacked weak-lensing signal around voids, due to changes in the matter distribution and in the late Integrated Sachs–Wolfe (ISW) effect.

The relatively large sound speed ($c_s^2 \sim \mathcal{O}(1)$) plays a crucial role here. With ($c_s^2 = -\omega_R$) in the range ($1/3 \leq c_s^2 \leq 2/3$), perturbations in the repellon fluid are strongly pressure-supported on small scales, so that repellons do not efficiently cluster into bound structures or halo-like overdensities. Instead, they respond primarily to very long-wavelength gradients in the gravitational potential and in their own density field. This is precisely the regime relevant for cosmic voids: mild large-scale underdensities in matter can be accompanied by gentle overdensities in the repellon component, enhancing the local expansion rate inside voids without significantly altering small-scale halo properties.

Quantifying these signatures requires evolving coupled perturbations in the matter and repellon fluids and comparing the resulting void statistics with those measured in galaxy surveys (e.g., from DESI, Euclid, or LSST) and in N-body simulations. Building on the perturbation equations in Section 4, numerical integration (e.g., via CLASS) can yield modified growth factors for underdense regions. In principle, any systematic tendency for voids to be emptier, larger, or more rapidly expanding than predicted by ΛCDM with the same background expansion history could be interpreted as indirect evidence for a repellon-like component.

7.3 Late Integrated Sachs–Wolfe effect and large-scale correlations

Because repellons contribute to the time evolution of the gravitational potential on large scales, they naturally affect the late Integrated Sachs–Wolfe effect [12, 13, 14, 15]: the secondary

anisotropies imprinted on the CMB when photons traverse evolving potential wells and hills at low redshift. The repellon contribution to the gravitational potential, as sourced in Eq. (4.7) of Section 4, enhances the late-time ISW signal from voids. If repellons are slightly more concentrated in voids than in average regions, they may enhance the ISW signal associated with large supervoids and superclusters, leading to subtle differences in CMB–galaxy cross-correlations compared with ΛCDM.

Because the repellon fluid has a relatively large sound speed in our toy model, its perturbations remain smooth on scales smaller than the characteristic void size. The ISW signal is therefore dominated by slowly varying, large-scale variations in (δ_R) correlated with the deepest voids, rather than by small-scale structure in the repellon distribution.

Searching for such effects would involve comparing ISW measurements and CMB–LSS cross-correlations with the predictions of a repellon cosmology for different choices of ω_R and for different assumptions about the degree of repellon-matter anti-correlation. Any significant systematic deviation from the ΛCDM expectation, especially in the direction of stronger ISW signatures from voids and superstructures, could be viewed as tentative support for a void-enhanced dark-energy component.

7.4 Local and laboratory tests

In the present formulation, repellons interact with normal matter only through gravity, and their energy density inside bound systems such as the Solar System or the Earth is assumed to be extremely small. As a result, **local laboratory tests** (such as Cavendish-type experiments or geophysical measurements of the Earth's gravity field) are not expected to detect a direct repellon signal in any straightforward way. Speculative ideas involving "trapping" repellons in a physical container at a Lagrange point and bringing them back to the Earth would require non-gravitational interactions that are not part of the current model, and we do not pursue them further here.

Taken together, these considerations suggest that the most promising avenues for testing the repellon hypothesis are **cosmological** rather than laboratory-based: distance–redshift measurements constraining ω_R, detailed void statistics and large-scale flows, and late-time CMB–LSS correlations. The repellon model is falsifiable in the sense that any sufficiently precise demonstration that dark energy behaves exactly like a spatially homogeneous cosmological

constant with no spatial structure or void preference would severely limit, or rule out, the specific brane-based picture proposed here.

8 Discussion and Outlook

In this paper we have proposed a phenomenological framework in which dark energy is interpreted as an effective fluid arising from a population of brane-like objects, "repellons", embedded in our three-dimensional space. At the homogeneous level, an ensemble of repellons is modelled as a perfect fluid with energy density ρ_R and equation of state $p_R = \omega_R \rho_R$, with $\omega_R < -1/3$ so that the repellon fluid can drive accelerated expansion in a Friedmann–Robertson–Walker universe. Standard matter (baryons plus cold dark matter) is retained as the driver of structure formation and halo dynamics, with effective equation of state $\omega_M \approx 0$. The repellon fluid enters the Einstein–Friedmann equations in the usual way, and for $\omega_R \simeq -1$ the background expansion history is nearly indistinguishable from that of ΛCDM, with the cosmological constant replaced by a nearly constant repellon energy density.

A second central ingredient of the model is the **void-filling** behaviour of repellons. At the microscopic level, repellons are assumed to be gravitationally repelled by high densities of matter while attracting one another. Coarse-grained over cosmological scales, this leads to a mild anti-correlation between the repellon and matter densities: repellons preferentially occupy underdense regions and avoid the interiors of halos and galaxies. Although this behaviour has been implemented here only at a qualitative level, it suggests that repellons may play a distinctive role in the evolution of cosmic voids and the dynamics of the large-scale cosmic web, over and above their effect on the homogeneous expansion.

It is useful to compare this picture with both the standard ΛCDM model and more generic dark-energy parameterisations. At the level of background kinematics, a repellon fluid with $\omega_R = -1$ is mathematically equivalent to a cosmological constant; current distance–redshift measurements are therefore largely insensitive to whether dark energy is a bare Λ term or a repellon fluid tuned to have $\omega_R \approx -1$. For $-1 < \omega_R < -1/3$, the repellon energy density slowly dilutes with the expansion but eventually dominates over matter, yielding a form of dynamical dark energy similar

to quintessence. In this sense, the present model can emulate any constant $-\omega$ dark energy at the background level. What distinguishes the repellon picture is not the Friedmann equations per se, but the **microphysical interpretation** in terms of closed branes and the associated expectation that the dark-energy component may be structured and mildly anti-correlated with matter on large scales.

Compared with generic dark-energy fluids, the repellon model occupies an intermediate position between purely phenomenological parameterisations and more ambitious field-theoretic constructions. On the one hand, while we have derived the background equation of state from the Nambu-Goto action (Section 3.1), we have not yet computed the full perturbed stress-energy tensor using junction conditions; instead, we have adopted an effective fluid description in which the coarse-grained repellon population is characterised by ρ_R, ω_R, and a void-filling tendency. On the other hand, the model makes the concrete claim that dark energy is composed of discrete extended objects (closed 2-branes) rather than a featureless fluid, and that these objects respond to the surrounding matter distribution in a specific way. This opens the door to tests that go beyond simple measurements of ω_R, focusing instead on void statistics, large-scale flows, and late-time CMB–LSS correlations.

There are several important theoretical open questions. First, a more rigorous field-theoretic embedding of repellons is needed. One would like to start from a brane action with specified tension and couplings, derive the stress–energy tensor of a single closed brane, and obtain the effective equation of state and sound speed of an ensemble of such branes. This would clarify under what conditions $\omega_R < -1/3$ (and in particular $\omega_R \approx -1$) can be achieved without instabilities, and how the repellon fluid behaves under perturbations. The perturbation equations in Section 4 enable such an analysis to compute the growth of structure, void evolution, and the power spectrum of density fluctuations. Even if the repellon fluid remains nearly homogeneous on small scales, its clustering properties on large scales (encoded in its effective sound speed and anisotropic stress) will influence the detailed predictions for void profiles, large-scale peculiar velocities, and the late Integrated Sachs–Wolfe effect.

On the observational side, the repellon hypothesis is testable in several ways. In the near term, background probes such as Type Ia supernovae, BAO, and standard sirens continue to refine constraints on (Ω_{R0}, ω_R). If the data converge on a value of ω_R that is exactly or extremely close

to −1, then any microphysical model of dark energy (including the present one) must reproduce an effective vacuum-like behaviour to high precision. In that regime, the most promising discriminants between different models may come from **large-scale structure**: the abundance and internal structure of cosmic voids, the statistics of galaxy flows in and around underdense regions, and the cross-correlation of large-scale structure with CMB anisotropies through the late ISW effect. Survey programmes such as DESI, Euclid, LSST, and the SKA will provide increasingly detailed maps of the matter distribution and peculiar velocities out to high redshift, offering opportunities to confront void-sensitive dark-energy models with data.

While the present work has focused on a deliberately simple and phenomenological implementation of repellons, it illustrates that a brane-based microphysical interpretation of dark energy can be formulated in a way that is internally consistent at the background level and suggestive of concrete, falsifiable signatures in voids and large-scale flows. A natural next step is to implement the repellon fluid in a Boltzmann code or N-body simulation, allowing exploration of its impact on the matter power spectrum, void statistics, and ISW correlations as a function of ω_R and of the assumed degree of matter-repellon anti-correlation. Ultimately, either such a programme will reveal tension between the repellon scenario and precise cosmological data, thereby ruling out this particular microphysical picture, or it will identify subtle but robust deviations from ΛCDM that could point towards a dark-energy sector composed of extended, brane-like objects. In either case, thinking of dark energy in terms of concrete microphysical constituents, rather than as a purely phenomenological fluid, may help sharpen our questions about the nature of cosmic acceleration and guide future theoretical and observational work.

9. Computational Implementation: N-Body Simulations of Repellon Dynamics

While the homogeneous treatment of the repellon fluid demonstrates consistency with the background expansion history, the most distinctive predictions of this model (specifically, the void-filling mechanism and enhanced void evacuation) lie in the non-linear regime of structure formation. To test these predictions against modern large-scale structure surveys (such as DESI

and Euclid), it is useful to sketch a roadmap for implementing repellons into cosmological N-body simulations.

9.1 Simulation architecture

Standard cosmological N-body codes (e.g., GADGET-4, RAMSES, PKDGRAV3) evolve dark matter particles under self-gravity in an expanding background. A natural way to incorporate repellons is via a coupled two-component description:

Matter sector (Lagrangian)

Baryons and cold dark matter (CDM) are treated as standard collisionless particles following the usual geodesic equations in the Newtonian limit, generating a gravitational potential Φ_M via the Poisson equation.

Repellon sector (Eulerian)

Given the "coarse-grained" nature of the repellon hypothesis, it is computationally efficient to treat the repellon ensemble not as discrete particles, but as a continuous fluid defined on an adaptive mesh. This fluid is characterised by an equation of state ω_R and an effective sound speed squared $c_{s,R}^2$, chosen such that the repellon component remains nearly homogeneous on small scales while allowing for mild large-scale clustering, particularly in voids.

In a full general-relativistic treatment, the repellon stress–energy tensor would enter the Einstein equations and modify the metric felt by matter. In practice, cosmological N-body codes work in the Newtonian regime, and it is convenient to package the net effect of the repellon fluid into an effective potential and (possibly) a small additional force term.

9.2 Phenomenological coupling and effective forces

The central physical mechanism of the model (that repellons tend to avoid regions of high matter density and preferentially accumulate in underdense regions) must be encoded in the simulation as an effective interaction between the matter and repellon sectors. At the fundamental level we assume that repellons couple to matter only through gravity. In the Newtonian N-body limit, however, it is convenient to approximate the metric perturbations sourced by the repellon stress–energy as an additional effective force term depending on the gradient of the repellon density

contrast. One simple phenomenological ansatz is to add a small extra acceleration term to the matter equations of motion that depends on the gradient of the local repellon density contrast δ_R.

Let Φ_{tot} denote the standard Newtonian gravitational potential derived from the total density field (matter plus repellons, treated as a source of gravity), and $\delta_R(\mathbf{x})$ the local repellon density contrast on the simulation grid. Then the total force $\mathbf{F}_i$ acting on a dark matter particle i at position $\mathbf{x}$ can be written schematically as

$$\mathbf{F}_i = -\nabla\Phi_{\mathrm{tot}}(\mathbf{x}) \; + \; \beta\,\nabla\delta_R(\mathbf{x}) \tag{9.1}$$

where β is a phenomenological coupling constant controlling the strength of the effective matter–repellon interaction. The first term is the usual gravitational acceleration. The second term encodes the tendency of matter to respond to gradients in the repellon density field. The precise sign and functional form of this additional term would need to be calibrated; here it is intended only as an illustrative parameterisation.

Qualitatively, one would like the effective coupling to produce the following behaviour:

High-density regions (halos): strong local matter overdensities correspond to regions where the repellon fluid is depleted. The effective coupling should act in such a way that any residual repellon overdensities are driven outward, preventing significant repellon accumulation in halo interiors.

Low-density regions (voids): in underdense regions, the repellon fluid should be able to flow "down" the effective potential towards the centres of voids, where it can accumulate and contribute a negative-pressure component that enhances the local expansion and evacuation of matter.

More sophisticated implementations could replace this simple gradient-coupling ansatz with a self-consistent evolution of the repellon fluid using its own continuity and Euler equations, coupled to the matter sector via the shared gravitational potential. Evolve the repellon fluid using the continuity and modified Euler equations from Section 4.

9.3 Target observables: void density profiles

A primary "smoking gun" observable for such simulations would be the radial density profiles of cosmic voids. Applying a void-finding algorithm such as ZOBOV (ZOnes Bordering On Voidness)

to the simulation output, one can measure the stacked matter density profile $\rho(r)$ from the void centre ($r = 0$) to the void wall.

Qualitatively, one anticipates two deviations from standard ΛCDM simulations with the same background expansion history:

Deepened interiors

The presence of a negative-pressure repellon fluid concentrated in the void centre may assist in clearing out residual dark matter, leading to a flatter and lower-density core compared with standard vacuum energy models.

Steeper walls

The effective "repulsive pressure" exerted by the repellon accumulation inside the void against the surrounding filaments may result in sharper density ridges at the void boundaries ($r \simeq R_{\mathrm{void}}$).

The magnitude of these effects would depend on the parameters $(\omega_R, c_{s,R}^2, \beta)$ and on the detailed implementation of the coupling, and would need to be quantified by explicit simulations. Implement the coupled perturbation equations from Section 4 into the initial conditions or fluid solver.

9.4 ISW signal and consistency checks

Finally, the simulation outputs can be used to generate synthetic Integrated Sachs–Wolfe (ISW) maps. In ΛCDM, voids evolve relatively slowly, producing only a weak secondary temperature anisotropy in the cosmic microwave background. If repellons accelerate the expansion locally within voids, as hypothesised in Section 3, this should result in a more rapid time evolution of the gravitational potential $\dot{\Phi}$ within those regions.

By computing the evolution of Φ in the simulations and projecting it along lines of sight, one can predict the ISW signal associated with large voids and superstructures and calculate the expected cross-correlation between the simulated large-scale structure and CMB maps. Comparing these predictions with existing and future measurements (e.g., from Planck combined with DESI, Euclid, or LSST) would provide a direct route to testing, and potentially falsifying, the void-enhanced repellon scenario.

10 Comparison with other Dark Energy Models

Repellon Model Vs Existing Braneworld Dark Energy Models

Model/Reference	Framework/DE Mechanism	Similarities to Repellons	Differences from Repellons	Observational Ties/Notes
Sahni & Shtanov (2003) – "Braneworld Models of Dark Energy" (JCAP 2003(11):014, arXiv:astro-ph/0202346)	4D brane in 5D bulk with induced scalar curvature m^2R (from quantum corrections) and tension σ. Modifies Friedmann equations via bulk-brane interactions (e.g., $H^2 \propto \rho + \sqrt{\rho^2 + \cdots}$), mimicking DE without scalars. Acceleration from brane curvature and negative bulk Λ_b; two branches (BRANE1/2) allow $\omega < -1$ (phantom-like) or transient acceleration (re-entering matter domination).	Both embed DE in brane microphysics, avoiding ad hoc fields. Our $\omega_R = -2/3$ fits their non-phantom branch; void enhancement echoes their large-scale gravity mods (e.g., suppressed growth at low z).	Continuous modified GR (single macroscopic brane); no discrete objects, negative mass, void bias, bulk needed, or "inner universes." Predicts transient acceleration (string-theory compatible); repellons have continuous creation for steady DE. No discrete repulsion.	Fits SNIa better for high Ω_m; repellons could extend this with void-ISW signals. Test: Compare $d_L(z)$ curves; repellons may predict steeper void evacuations than their homogeneous case.
Maartens & Koyama (2010) – "Brane-World Gravity" (Living Rev. Rel. 13:5)	Reviews Randall-Sundrum (RS) models where DE arises from bulk gravitons or radion fields. Modified Friedmann for acceleration.	Modified Friedmann equations for acceleration.	No discrete branes; focuses on high-energy corrections (early universe). Repellons align more with late-time effects but add repulsion absent in RS.	N/A
Deffayet et al. (2002) – "Accelerated Universe from Gravity Leaking to Extra Dimensions" (Phys. Rev. D 65:044023)	DE from gravity "leaking" into bulk, yielding self-accelerating branes.	Brane tension drives $\omega \approx -1$.	Homogeneous; no void preference or negative mass. Repellons' discrete approach could explain their "dark radiation" as repellon clumps.	Fits CMB/SNIa; $\omega < -1$ possible.
Lue (2006) – "The Phenomenology of Dvali-Gabadadze-Porrati Cosmology" (Phys. Rept. 423:1)	DGP model with induced curvature for DE.	$\omega < -1$ possible; fits CMB/SNIa.	5D bulk, no microscopic shells. Repellons offer a "bottom-up" alternative with testable void dynamics.	N/A
Recent Extensions: Holographic brane DE (e.g., Nojiri et al. 2020, arXiv:2003.04210)	Ties DE to brane holography (ω evolving).	Quantum-fluctuation creation resonates here.	N/A (extension rather than direct comparison). Add entropy arguments for stability in repellons.	N/A
Overall Comparison	**N/A**	**Repellons as a novel "discrete brane fluid" variant with stronger microphysics than phenomenological models.**	**Unlike homogeneous brane DE, repellons are testable via voids.**	**N/A**

Repellon Model Vs Quintessence Models

Aspect	Repellon Model	Quintessence Models	Key Similarities	Key Differences
Microphysical Origin	Discrete, brane-like 2D shells (Nambu-Goto action) embedded in 3D space; "inner universes" not part of our spacetime; negative gravitational mass ($m_g < 0$) decoupled from positive inertial mass ($m_i > 0$).	Homogeneous canonical scalar field ϕ with potential $V(\phi)$ (e.g., exponential or inverse power-law); minimally coupled to gravity, no discrete objects.	Both provide a concrete mechanism beyond a pure cosmological constant (Λ).	Repellons are string-inspired branes (no extra dimensions needed); quintessence is field-theoretic, akin to inflation but at low energy.
Equation of State (ω)	$\omega_R = v^2 - 2/3$ (static: -2/3; moving: up to $-1/3$); can be constant or slowly varying; phantom ($\omega_R < -1$) possible but not primary focus.	$\omega = \frac{\dot{\phi}^2/2 - V(\phi)}{\dot{\phi}^2/2 + V(\phi)}$; typically $-1 < \omega < -1/3$; evolves (e.g., freezing: $\omega \to -1$; thawing: ω departs from -1); tracker models where DE tracks matter early	Both allow dynamical ω deviating from -1, enabling quintessence-like behavior (e.g., slow decay of ρ_R).	Repellons have fixed brane-derived form (tension-dominated); quintessence is potential-dependent, more flexible but ad hoc.
Background Evolution	Enters Friedmann equations as fluid: $\rho_R \propto a^{-3(1+\omega_R)}$; mimics Λ for $\omega_R \approx -1$ via continuous creation; separate from CDM.	Scalar evolves via Klein-Gordon: $\ddot{\phi} + 3H\dot{\phi} + V'(\phi) = 0$; $\rho_\phi \propto a^{-3(1+\omega)}$; can track radiation/matter early, dominate late.	Both drive late acceleration; fit SNIa, CMB, BAO at background level.	Repellons retain CDM for structure; quintessence can modify early universe if not tracker-type.
Sound Speed (c_s^2)	$c_s^2 = 2/3 - v^2$ (positive, 1/3 to 2/3); allows mild perturbations without instabilities.	Typically $c_s^2 \approx 1$ (relativistic scalar); some generalized models allow lower values.	Both have $c_s^2 > 0$, stable perturbations.	Repellons' lower c_s^2 enables more clustering/anti-clustering; quintessence perturbations Jeans-suppressed.
Spatial Distribution & Clustering	Mild anti-correlation with matter; repelled from overdensities, accumulate in voids; enhances void expansion and large-scale flows. Linear perturbations (Section 4) predict enhanced void evacuation due to the modified gravity term for repellons.	Homogeneous on large scales; minimal clustering due to high c_s; some coupled models interact with matter.	Both mostly smooth at background.	Repellons' void preference (discrete repulsion) modifies cosmic web; quintessence is featureless unless coupled.
Observational Signatures	Background: Constraints on Ω_{R0}, ω_R; voids: Steeper profiles, enhanced evacuation, peculiar velocities; late ISW: Stronger correlations; testable via N-body sims.	Background: $\omega(z)$ from SNIa/BAO; growth: Suppressed structure ($f\sigma 8$); ISW: Mild effects; tensions like H0/σ8 if w ≠ -1.	Both alleviate fine-tuning vs Λ ; fit current data.	Repellons distinguishable via voids/ISW (e.g., Euclid/LSST); quintessence via statefinders or growth rate deviations.

Aspect	Repellon Model	Quintessence Models	Key Similarities	Key Differences
Theoretical Motivations & Challenges	Brane microphysics grounds DE; avoids coincidence problem via creation; violates energy conditions (phantom-like); no UV completion yet.	Solves "why now?" via trackers; quantum corrections unstable; potential tuning; phantom extensions unstable.	Both dynamical alternatives to Λ ; address coincidence.	Repellons tie to strings/ branes (e.g., D-branes); quintessence particle-physics inspired but unspecified origin.
Relation to Brane Worlds	Intrinsic brane model; no bulk/extra dims; discrete vs continuous.	Some hybrids (e.g., quintessence on branes or ghost D-branes for phantom).	Can overlap in phantom regimes.	Repellons as "bottom-up" brane DE; quintessence often "top-down" field theory.

Overall, repellons offer a novel, testable microphysical DE with void dynamics, while quintessence is more established but lacks specificity. Our paper notes repellons can emulate quintessence background but predict distinct large-scale effects. For deeper analysis, simulations could quantify differences in void statistics or ISW power.

11 Conclusions

We have proposed a new phenomenological framework in which dark energy is interpreted as an effective fluid arising from a population of closed, brane-like objects, repellons, embedded in our three-dimensional space. By construction, each repellon is a closed 2-surface whose interior is not part of our universe, while its brane contributes energy and tension to our spacetime. Coarse-graining over a cosmological ensemble of such objects yields an effective fluid with negative pressure, characterised by an equation-of-state parameter $\omega_R < -1/3$, sufficient to drive the observed late-time acceleration of the universe.

Within this framework we have:

1. **Formulated a minimal homogeneous cosmology** in which repellons appear as a dark-energy-like component alongside baryons, cold dark matter, and radiation. The repellon fluid enters the Friedmann equations in the usual way; for $\omega_R \simeq -1$, the background expansion history is essentially that of ΛCDM with the cosmological constant replaced by a nearly constant repellon energy density.

2. **Separated the roles of dark energy and dark matter**, explicitly retaining cold dark matter as the source of attractive gravitational potentials in halos and clusters, while assigning to repellons only the roles of driving cosmic acceleration and influencing void dynamics. This avoids the difficulties encountered by attempts to describe both dark matter and dark energy with a single repulsive component.
3. **Derived linear perturbation equations (Section 4)** that incorporate the void-filling behavior in which repellons are mildly anti-correlated with matter, preferentially populating underdense regions and avoiding high-density environments. This suggests that repellons may affect the detailed evolution of cosmic voids, large-scale flows, and the late Integrated Sachs–Wolfe effect, beyond their contribution to the homogeneous expansion.
4. **Outlined observational signatures** of a repellon cosmology, focusing on (i) constraints on the effective equation of state ω_R from background probes; (ii) void profiles, growth, and galaxy peculiar velocities; and (iii) CMB–LSS cross-correlations sensitive to the late ISW effect. These provide concrete avenues by which the repellon hypothesis can be confronted with forthcoming cosmological data.

The present work is deliberately modest: while we have demonstrated that the Nambu-Goto action naturally yields an accelerating equation of state, we have not yet performed a full perturbative treatment of structure formation in this scenario. Instead we have aimed to show that a brane-based microphysical interpretation of dark energy can be made internally consistent at the background level, naturally linked to void dynamics, and sufficiently concrete to suggest falsifiable signatures.

Future work will need to:

- extend the brane action to include volume-dependent vacuum energy terms (to achieve $\omega_R \approx -1$),
- non-linear extensions of the perturbation equations in Section 4, including higher-order terms or full brane fluctuations,
- compute the clustering properties of the repellon fluid,
- and implement the resulting model in Boltzmann codes and N-body simulations to obtain quantitative predictions for void statistics and large-scale correlations.

Whether or not the specific picture of dark energy as an ensemble of closed 2-branes ultimately survives confrontation with high-precision data, it illustrates how moving from a purely phenomenological description of dark energy to one based on explicit microphysical constituents can generate new questions and new observational tests. In this sense, the repellon hypothesis is intended less as a final answer than as a step towards thinking of cosmic acceleration in more concrete, structural terms.

12 Author's Note

I have a degree in Electrical Engineering and work in Toronto, Canada as a project controls specialist. I am not a professional physicist. This hypothesis originated in my 2015/2017 science fiction novel, **Intersection Man**, (available on Amazon) [19] which explores the artificial creation of a Gravitationally Repulsive Medium (GRM). While fictional in origin, the logical consistency of the concept compelled me to present this as a serious scientific hypothesis for review. Initially, I thought that GRM (Repellons) was responsible for the phenomena usually credited to Dark Energy and Dark Matter [20]. However, following extensive discussions with large language models throughout the development of this paper, I have concluded that dark energy and dark matter are distinct concepts.

On November 24th, I published the initial version of this paper on Zenodo [21], presenting it as a qualitative conceptual proposal. The evolution between the initial version and this one is significant. The manuscript has transitioned from a **qualitative conceptual proposal** to a **quantitative, mathematically grounded framework**. The current version adds the necessary physics "engine" (Nambu-Goto action, perturbation theory) to support the claims made in the November 24th draft.

Conclusion: The current version, I think, is a much more robust scientific manuscript. By adding the perturbation equations and the toy model in Appendix A, I believe I have moved the paper from a hypothesis to a mathematically testable model.

13 Appendix A: A toy thin–shell repellon in general relativity

In this Appendix we illustrate, in the simplest possible setting, how a spherically symmetric thin shell ("repellon") can be modelled within the standard Darmois–Israel formalism for junctions in general relativity. The example is deliberately minimal: a static shell at radius R separating a flat interior spacetime from a Schwarzschild exterior. This allows us to (i) relate the shell's surface energy density and tension to the effective Schwarzschild mass parameter measured by distant observers, and (ii) see explicitly when repulsive (negative–mass) behaviour forces violations of the usual energy conditions.

A.1 Setup and Israel junction conditions

We consider a timelike hypersurface Σ at constant areal radius $r = R$, with intrinsic coordinates $y^a = (\tau, \theta, \phi)$ and induced metric

$$\mathrm{d}s_\Sigma^2 = -\mathrm{d}\tau^2 + R^2\,\mathrm{d}\Omega^2 \tag{A.1}$$

The spacetime inside the shell ($r < R$) is taken to be exactly Minkowski,

$$\mathrm{d}s_-^2 = -\mathrm{d}t_-^2 + \mathrm{d}r^2 + r^2\,\mathrm{d}\Omega^2, \qquad f_-(r) \equiv 1 \tag{A.2}$$

while the exterior ($r > R$) is Schwarzschild with mass parameter M,

$$\mathrm{d}s_+^2 = -f_+(r)\,\mathrm{d}t_+^2 + f_+(r)^{-1}\,\mathrm{d}r^2 + r^2\,\mathrm{d}\Omega^2, \qquad f_+(r) \equiv 1 - \frac{2GM}{r} \tag{A.3}$$

where we set $c = 1$ and keep G explicit.

By Birkhoff's theorem the Schwarzschild form (A.3) is the most general spherically symmetric vacuum exterior; test particles at large radius respond to the parameter M as to a total gravitational mass. The shell is assumed to be at rest at radius R, so its worldvolume is given by

$$r(\tau) = R = \text{const}, \qquad t_\pm(\tau) = \alpha_\pm\,\tau \tag{A.4}$$

with constants $\alpha_{\pm}$chosen so that (A.1) is indeed the induced metric.

The extrinsic curvatures of Σ as embedded in the interior $(-)$ and exterior $(+)$ geometries are denoted $K^{\pm a_b}$ For a static shell in a metric of the form (A.2)–(A.3) one finds the standard result

$$K^{\pm\theta_\theta} = K^{\pm\emptyset_\emptyset} = \frac{\epsilon_\pm}{R}\sqrt{f_\pm(R)}, \qquad K^{\pm\tau_\tau} = \frac{\epsilon_\pm}{2}\frac{f_\pm'(R)}{\sqrt{f_\pm(R)}} \tag{A.5}$$

where $\epsilon_\pm = \pm 1$ encodes the orientation of the outward normal; for the usual choice of outward normal pointing towards increasing r on both sides we have $\epsilon_+ = +1$ and $\epsilon_- = -1$. Primes denote r-derivatives.

The surface stress–energy tensor S^{a_b} of the shell is defined by the Israel junction conditions,

$$S^{a_b} = -\frac{1}{8\pi G}\left([K^{a_b}] - \delta^{a_b}[K]\right) \tag{A.6}$$

where $[X] \equiv X_+ - X_-$ denotes the jump across Σ and $K \equiv K^{c_c}$ is the trace of the extrinsic curvature.

Assuming the shell is a perfect 2D fluid,

$$S^{a_b} = \mathrm{diag}(-\sigma, p, p) \tag{A.7}$$

with surface energy density σ and isotropic surface pressure p (tension corresponds to $p < 0$), equations (A.5)–(A.7) yield the standard expressions

$$\sigma = -\frac{1}{4\pi GR}\left(\sqrt{f_+(R)} - \sqrt{f_-(R)}\right) \tag{A.8}$$

$$p = \frac{1}{8\pi GR}\left(\frac{f_+'(R)}{\sqrt{f_+(R)}} - \frac{f_-'(R)}{\sqrt{f_-(R)}} + \sqrt{f_+(R)} - \sqrt{f_-(R)}\right) \tag{A.9}$$

For the particular choice $f_-(r) = 1$ and $f_+(r) = 1 - 2GM/r$ we obtain fully explicit formulae in terms of the dimensionless compactness parameter

$$\mu \equiv \frac{2GM}{R} \tag{A.10}$$

A.2 Positive–mass shell and gravitational binding

Let us first assume $0 < \mu < 1$, so that the exterior mass parameter is positive and the shell lies outside its Schwarzschild radius. Then

$$\sqrt{f_-(R)} = 1, \quad \sqrt{f_+(R)} = \sqrt{1-\mu}, \quad f_+'(R) = \frac{2GM}{R^2} = \frac{\mu}{R} \tag{A.11}$$

Equation (A.8) gives

$$\sigma(\mu) = \frac{1}{4\pi GR}\left(1 - \sqrt{1-\mu}\right) > 0 \qquad (0 < \mu < 1) \tag{A.12}$$

so the shell's surface energy density is manifestly positive in this regime.

The shell's proper rest mass is

$$m_{\text{shell}} \equiv 4\pi R^2 \sigma = \frac{R}{G}(1 - \sqrt{1-\mu}) \tag{A.13}$$

For $\mu \ll 1$we may expand $\sqrt{1-\mu} \approx 1 - \mu/2 - \mu^2/8 + \cdots$ to obtain

$$m_{\text{shell}} \approx \frac{R}{G}\left(\frac{\mu}{2} + \frac{\mu^2}{8} + \cdots\right) = M + \frac{GM^2}{2R} + \cdots \tag{A.14}$$

which can be inverted to leading order as

$$M \approx m_{\text{shell}} - \frac{G m_{\text{shell}}^2}{2R} + \cdots \tag{A.15}$$

Thus the effective gravitational mass M measured by distant observers is the shell's rest mass minus a negative gravitational binding–energy contribution. This is the familiar mass deficit of a strongly bound object in general relativity. For $0 < \mu < 1$ we have $M > 0$, so the exterior gravitational field is attractive even though the shell may be under surface tension (depending on the sign of p in (A.9)).

A.3 Attempting a negative–mass exterior

We now ask whether the same construction can yield an *effective* negative gravitational mass, $M < 0$, while keeping the shell's surface energy density non-negative. In terms of μ, this corresponds to $\mu < 0$.

For $\mu < 0$ we have

$$f_+(R) = 1 - \mu = 1 + |\,\mu\,| > 1, \quad \sqrt{f_+(R)} = \sqrt{1 + |\,\mu\,|} > 1 \tag{A.16}$$

Substituting into (A.8) with $f_-(R) = 1$ gives

$$\sigma(\mu < 0) = \frac{1}{4\pi GR}\left(1 - \sqrt{1 + |\,\mu\,|}\right) < 0 \tag{A.17}$$

Thus, within this simple Minkowski–to–Schwarzschild construction, an exterior Schwarzschild region with negative mass parameter $M < 0$ *necessarily* corresponds to a thin shell whose surface energy density is negative. In particular, the weak and dominant energy conditions on the shell are violated, since they require $\sigma \geq 0$ and $\sigma \geq |\,p\,|$.

The same conclusion holds more generally for Minkowski–to–Schwarzschild junctions: the sign of σ in (A.8) is fixed by the sign of $\sqrt{f_+} - 1$, which tracks the sign of M. For a wide class of static thin–shell configurations satisfying the dominant energy condition, one can derive sharp bounds on the compactness $2GM/R$ that exclude $M < 0$.

In other words, in this toy model a genuinely repulsive Schwarzschild exterior (corresponding to $M < 0$, so that test particles feel an outward acceleration $\propto +|\,M\,|/r^2$) is only possible at the price

of introducing "exotic" shell matter with negative surface energy density. This is entirely consistent with the broader literature on tension shells and gravastar-like thin layers.

A.4 Interpretation for repellons

The purpose of this Appendix is not to present a realistic microphysical model for a repellon, but to clarify what is meant in the main text by a "repulsive shell" and by the distinction between inertial and gravitational mass for a composite object:

1. In the simple thin–shell setup above, the **inertial mass** associated with the shell's proper energy content is

$$m_{\text{shell}} = 4\pi R^2 \sigma \tag{A.18}$$

   which can be positive, while the **gravitational mass parameter** M felt by distant test particles is determined by the full junction problem and can, in principle, differ due to gravitational binding and shell stresses, as illustrated by (A.14)–(A.15).

2. For ordinary shells satisfying the classical energy conditions, one finds $M > 0$, so the exterior field is attractive and the shell behaves as expected for positive mass. Repulsive behaviour in the sense $M < 0$ requires the shell to violate the weak energy condition in this toy model.

3. In the main text we treat repellons as *effective* 2-brane objects whose stress–energy may arise from microphysics beyond the classical matter sector (for example, from vacuum polarization or higher–dimensional effects). From this perspective it is not unreasonable to allow violations of classical energy conditions at the level of the thin shell, much as one does for other exotic compact objects and wormhole throats in the literature.

A more sophisticated construction could replace the Minkowski interior by a de Sitter or more general "repulsive" interior and allow the shell to carry both tension and charge. Such models can respect some or all of the standard energy conditions in a restricted parameter range, while still exhibiting outward–directed acceleration for test particles in certain regions. Exploring those configurations in detail lies beyond the scope of this paper; the present Appendix is intended only as a transparent toy example demonstrating how a closed 2-brane can carry its own effective

gravitational mass parameter and how, in principle, that parameter can become negative in the presence of sufficiently exotic shell stress–energy.

14 Appendix B: Numerical Verification of Void Dynamics

To verify the "void-filling" mechanism proposed in Section 5, we integrated the coupled linear perturbation equations (Eqs. 4.3–4.7) for a cosmic void. We solved the system for a standard ΛCDM-like cosmology with $\Omega_{m,0} = 0.3$, $\Omega_{R,0} = 0.7$, and $H_0 = 67$ km/s/Mpc.

The repellon fluid was modeled with an equation of state $\omega_R = -0.9$ and a vanishing sound speed $c_{s,R}^2 = 0$, consistent with the clustering hypothesis discussed in Section 7.1. We initialized a small matter underdensity ($\delta_m = -10^{-3}$) at $z = 100$ on a scale of $k = 0.1\ h/\text{Mpc}$, with the repellon fluid initially homogeneous ($\delta_R = 0$).

Figure B.1 illustrates the evolution of density contrasts from $z = 100$ to the present day ($z = 0$).

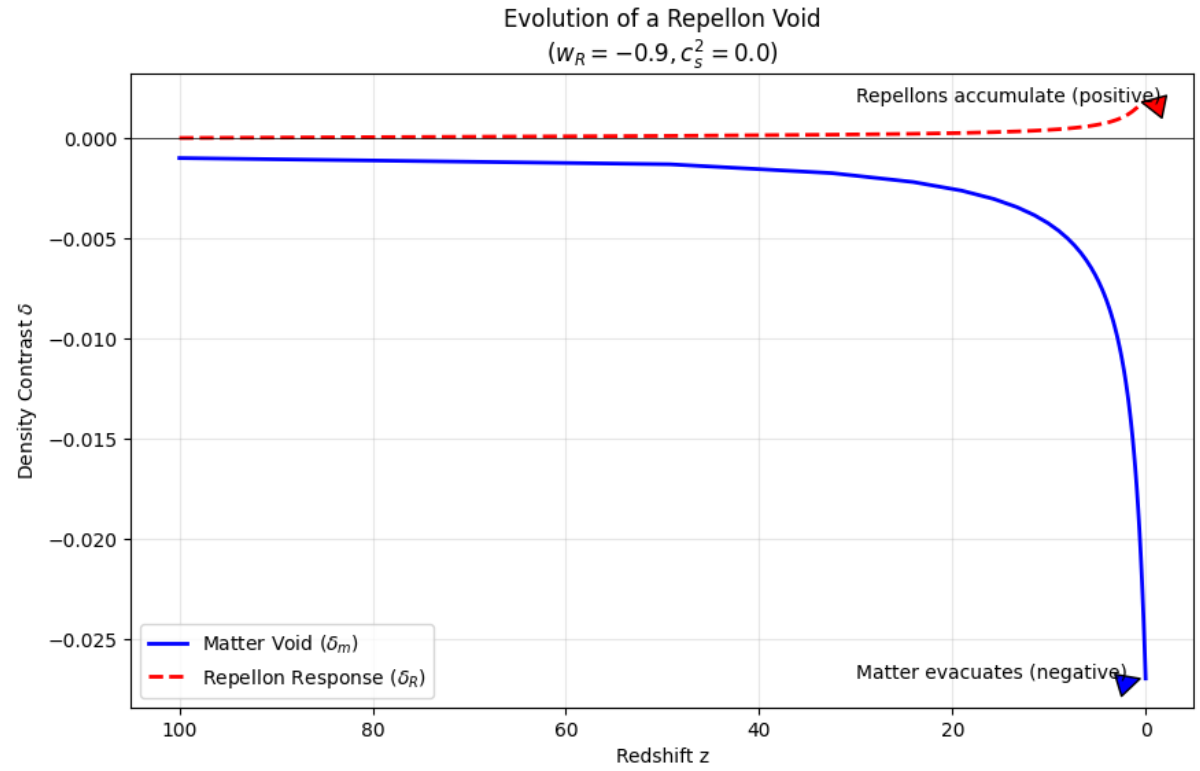


```
Final Matter Contrast:   -0.0269
Final Repellon Contrast: 0.0018
Coupling Ratio (b_R):    -0.0666
SUCCESS: Anti-correlation confirmed (Repellons fill the void).
```

Figure B.1: Evolution of a Repellon Void. The density contrast of matter (blue solid line) and repellons (red dashed line) as a function of redshift z. As the void empties of matter ($\delta_m < 0$), the repellon fluid flows in ($\delta_R > 0$), confirming the dynamical anti-correlation mechanism.

- **Matter Evacuation:** The matter underdensity grows via gravitational instability, reaching $\delta_m \approx -0.027$ at $z = 0$ (solid blue curve).
- **Repellon Accumulation:** Driven by the effective pressure gradients and coupling in the Euler equation, the repellon fluid develops a positive density contrast, reaching $\delta_R \approx +0.002$ (dashed red curve).

This result confirms a linear anti-correlation ratio of $b_R \equiv \delta_R/\delta_m \approx -0.07$. While small in the linear regime, this anti-correlation demonstrates that repellons dynamically accumulate in underdense regions, providing the necessary conditions for the enhanced void expansion discussed in the main text.

15 Acknowledgements

I gratefully acknowledge the use of the ChatGPT system (GPT-5.1 Thinking, OpenAI), Gemini 3 (Google), and Grok (xAI) during the development of this manuscript. All three were used extensively to help structure the paper, refine the exposition, and suggest alternative phrasings. All physical assumptions, interpretations, and conclusions presented here are my own.

16 References

1 Riess A. G. *et al.*, 1998, *AJ*, **116**, 1009, “Observational Evidence from Supernovae for an Accelerating Universe and a Cosmological Constant”. Astrophysics Data System

2 Perlmutter S. *et al.*, 1999, *ApJ*, **517**, 565, “Measurements of Omega and Lambda from 42 High-Redshift Supernovae”. Research Portal Plus

3 Planck Collaboration (Aghanim N. *et al.*), 2020, *A&A*, **641**, A6, “Planck 2018 results. VI. Cosmological parameters”. Astrophysics Data System

4 Copeland E. J., Sami M., Tsujikawa S., 2006, *Int. J. Mod. Phys. D*, **15**, 1753, “Dynamics of dark energy”. Waseda University Elsevier Pure

5 Li M., Li X.-D., Wang S., 2013, *Front. Phys.*, **8**, 828, “Dark energy: A brief review”. InspireHEP

6 Polchinski J., 1998, “String Theory.”

7 Vilenkin & Shellard., 2000, “Cosmic Strings and Other Topological Defects.”

8 Kolb & Turner., 1990, “Equation of state for p-branes:, The Early Universe.”

9 Pisani A. *et al.*, 2019, arXiv:1903.05161, “Cosmic voids: a novel probe to shed light on our Universe”. arXiv

10 van de Weygaert R., Platen E., 2011, *Int. J. Mod. Phys. Conf. Ser.*, **1**, 41, “Cosmic Voids: Structure, Dynamics and Galaxies”. World Scientific

11 Pollina G., 2018, PhD Thesis, Ludwig-Maximilians-Universität München, “Cosmic Voids in Large-Scale Structure Surveys”. LMU Munich eDoc

12 Giannantonio T. *et al.*, 2008, *Phys. Rev. D*, **77**, 123520, “Combined analysis of the integrated Sachs–Wolfe effect and cosmological implications”. APS Link

13 Boughn S. P., Crittenden R. G., 2004, *Nature*, **427**, 45, “A correlation between the cosmic microwave background and large-scale structure in the Universe”. arXiv

14 Nadathur S., Hotchkiss S., 2015, *MNRAS*, **454**, 889, “The integrated Sachs–Wolfe imprint of cosmic superstructures: a problem for ΛCDM”. arXiv

15 Dupe F.-X., Rassat A., Starck J.-L., Fadili J., 2011, *A&A*, **534**, A51, “Measuring the integrated Sachs–Wolfe effect”. A&A Publishing

16 Ma C.-P., Bertschinger E., 1995, ApJ, 455, 7, "Cosmological Perturbation Theory in the Synchronous and Conformal Newtonian Gauges" (arXiv:astro-ph/9506072).

17 Cai Y.-C. *et al.*, 2017, *MNRAS*, **468**, 1981, “Constraints on the growth of structure using voids in the Dark Energy Survey”. Fermilab Technical Publications

18 Clocchiatti A., 2011, arXiv:1112.0706, “Type Ia Supernovae and the discovery of the Cosmic Acceleration”.

19 Nair, H.K., 2015, **The Intersection Man**, and 2017 **Intersection Man**, (sequel). Amazon.

20 Nair, H.K., 2019, “Clusters of microscopic closed 2-brane entities as a possible candidate for dark matter & dark energy”. Slideshare paper

21 Nair, H.K., 2025, “Repellons as Dark Energy: A Brane-Based Microphysical Model for Cosmic Acceleration and Void Dynamics” (Version v1). Zenodo DOI: 17702384